Materials Science Forum Vols. 408-412 (2002) pp. 1573-1578

Oriented Growth of $LiNbO_3$ Thin Films for SAW Properties

V. Bornand[1], I. Huet[1], D. Chateigner[2] and Ph. Papet

[1] Laboratoire de Physicochimie de la Matière Condensée, Université Montpellier 2, LPMC, Place E. Bataillon C.C. 003, FR-34095 Montpellier Cedex 5, France

[2] Laboratoire de Cristallographie et Science des Matériaux, ISMRA, 6 Bd. du Maréchal Juin, FR-14050 Caen, France

Keywords: 2-Step Growth, Al_2O_3 Substrate, $LiNbO_3$, Lithium Niobate, Oriented Thin Films, Pyrosol, RF Sputtering, SAW Device, Si Substrates, Texture

Abstract. An original 2-step growth process was developed for the deposition of $LiNbO_3$ thin films onto <111>-Si and <001>-Al_2O_3 substrates. By combining both the r.f. sputtering and the pyrosol methods, stoichiometric <001>-oriented heterostructures could be achieved. Depositions performed on <111>-Si templates led to fiber textures, characteristic of oriented polycrystalline materials. <001>-Al_2O_3 substrates allowed the development of hetero-epitaxial layers, built up of two 60°-rotated domains. The mechanisms behind the in-plane orientation are discussed.

Introduction

There is a global interest in developing Surface Acoustic Wave (SAW) devices of high frequency capability, high power durability and zero temperature dependence of frequency. From application standpoint, lithium niobate has attracted much attention this last decade due to its unusual combination of ferroelectric, piezoelectric and acousto-optic coefficients [1]. $LiNbO_3$ (LN) thin films offer an enticing potential for high-frequency broad-band pass SAW device applications when deposited onto silicon [2], diamond-coated silicon [3,4] or Al_2O_3 [5] substrates.

In order to optimally benefit from the material properties, it is necessary to grow $LiNbO_3$ thin films with a preferred crystallographic orientation, *i.e.* for this phase with the c-axis normal to the surface of the substrate. For this purpose, a 2-step growth process has been developed which involves (1) creating a high-nucleation density by radio-frequency (r.f.) sputtering in the early stages of the film growth and (2) enhancing both the crystallinity and the preferential orientation by reactive chemical sputtering (also named pyrosol) [6]. This article summarizes our studies on the growth of $LiNbO_3$/<111>-Si and $LiNbO_3$/<001>-Al_2O_3 heterostructures. Emphasis is given on interface control to promote <001>-oriented crystallization process. Results from textural, microstructural and composition analyses are presented.

Material and Experimental Procedure

The difficulty often encountered in the nucleation of the LN material is attributed to the formation of an intermediate Li-deficient phase, namely $LiNb_3O_8$. During the initial growth stage, parameters such as interfacial energies are poorly known and bulk values are not valid in the first few monolayer regimes. However, for direct and controlled LN deposition, it has been shown that a high nucleation barrier must be overcome [7,8]. This can be achieved by the use of a growth template with a good lattice and structure matching. As recently reported, the ready formation of a thin weakly-crystallized LN layer by r.f. sputtering makes it a coherent template for the subsequent oriented growth of homogeneous LN thin films by pyrosol [6]. Experiments were performed at high temperatures to ensure the in-situ crystallization of the films, without post-annealing treatments.

The precise control of film development requires deposition operations under a set of optimum processing parameters, particularly when competitive phase types and elements of different volatility are present. A summary of the experimental parameters is presented in Table 1. The crystalline structure, morphology and chemical composition of such as-deposited films were investigated by X-ray diffraction (XRD), X-ray QTA, scanning electron microscopy (SEM), atomic force microscopy (AFM) and secondary ion mass spectroscopy (SIMS), respectively.

Table 1. Growth conditions for $LiNbO_3$ thin films deposited by a combined deposition process

Step 1: r.f. sputtered layer		**Step 2:** pyrosol deposited layer	
Targets	Sintered ceramics Li/Nb=1.4	**Precursors**	Li(AA) + $Nb(Et)_4$
		Solvent	Methanol
Gas	Mix Ar:O_2 (60:40)	**Solutions**	[Li]=10^{-2}mol/l – Li/Nb=1
Pressure	20 to 60 mTorr	**Spraying**	f=800kHz – P=70W
r.f. Power	100 W	**Carrier gas**	Dry and clean air
Temperature	600 to 625°C	**Temperature**	600 to 660°C

Results and Discussion

Under optimized conditions, c-preferentially oriented LN thin films can be deposited on both <111>-Si and <001>-Al_2O_3 substrates (Fig. 1), even though a minor <110>-second texture component can be seen on sapphire.

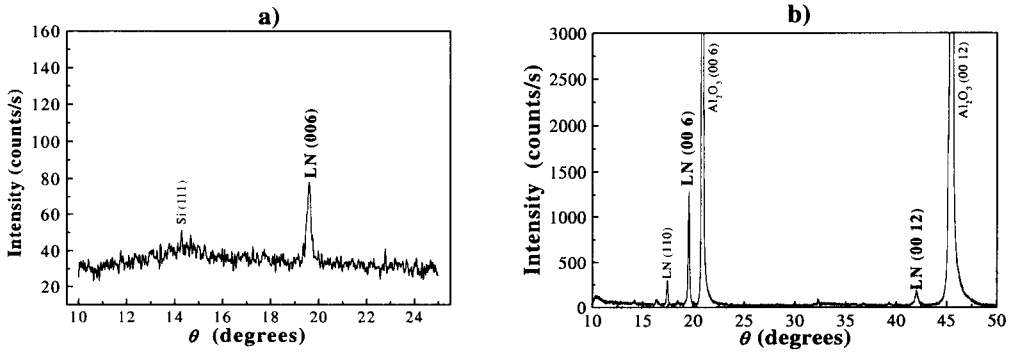

Fig 1. XRD spectra of $LiNbO_3$ thin films deposited on **(a)** <111>-Si and **(b)** <001> Al_2O_3 substrates.

Such as-deposited samples exhibit steep interfaces, with reduced interdiffusion phenomena and constant compositions through the overall film thickness (Fig. 2). In the present deposition process, the first weakly-crystallized sputtered film acts as a coherent buffer layer for the second pyrosol-deposited film, thus (1) enhancing the growth of highly-oriented crystallites and (2) limiting chemical interfacial reactions.

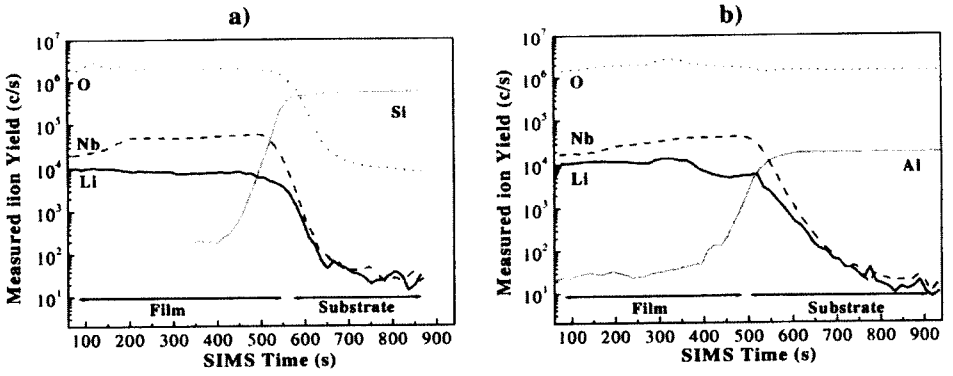

Fig 2. SIMS depth profile of ~300nm-thick $LiNbO_3$ thin films deposited on **(a)** <111>-Si and **(b)** <001> Al_2O_3 substrates.

Texture experiments using a 5° x 5° grid were carried out using the CPS 120 from INEL and the direct integration procedure as explained elsewhere [9]. A QTA was performed on both films using a WIMV refinement as implemented in Beartex [10], assuming cell parameters of the bulk (a = 0.515 nm, c = 1.386 nm, R3c space group), on the two pole figures {012}, {110} and {104} measured up to 70° in tilt angle with a measuring time of 2 min per point. We obtained RP_1 values of 4 % for LN/Si and 24 % for LN/Al_2O_3. The recalculated {001} and {100} pole figures are presented in Fig. 3. A strong orientation of the crystallites with a $c_\perp$ main component is developed in both heterostructures, reaching density values as high as 23 m.r.d. and 60 m.r.d. for LN/Si and LN/Al_2O_3, respectively. However, a complete out-of plane texturation could not be achieved neither on Si nor on Al_2O_3 substrates, $a_\perp$ and $<202>_\perp$, and a $<211>_\perp$ minor component being respectively present. The main difference between the two heterostructures rely in their in-plane orientation, as revealed by {100} pole figures.

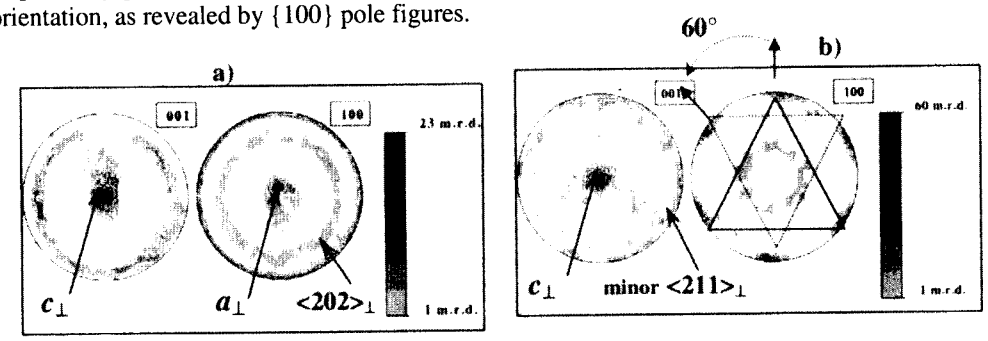

Fig 3. {001} and {100} pole figures, as recalculated from the orientation distribution function, of $LiNbO_3$ thin films deposited on **(a)** <111>-Si and **(b)** <001> Al_2O_3 substrates. Equal area projection, logarithmic scale, density levels above 1 m.r.d.

In the LN/Si film, all texture components are fiber-like (Fig. 3a). The film structure depends strongly on the initial growth stages. Crystallite orientation generally arises from either surface free energy or growth rate anisotropy [11]. LN is highly anisotropic and the c-axis is known to be one of the fastest growth direction [12]. Then, after nucleation of the <001>-oriented grains, they grow preferably at the expense of other grains as in a common growth mechanism. Besides, (111) planes in the FCC structure (Si substrate) are high-density ones, thus offering a large number of nucleation sites favorable for a dense and selected oriented growth. However, no coincidence site

lattice with reasonable matching of the parameters could be identified between LN and Si, and therefore there is no reason for any ordering in the plane, resulting in an axially symmetric texture.

On the contrary, hetero-epitaxial-like textures can be obtained on <001>-Al_2O_3 substrates, with a d-spacing mismatch of 5 % ($d_{\{110\}}(Al_2O_3)$ = 0.258 nm; $d_{\{200\}}(Si)$ = 0.271 nm), resulting in a stronger texture (F^2 = 101 m.r.d.^{2}) compared to the LN/Si sample (F^2 = 9.7 m.r.d.^{2}). Assuming a continuous oxygen sublattice at the interface between LN and Al_2O_3 ($R\bar{3}c$ space group), the 6-fold symmetry observed on the {100} pole figure (Fig. 3b) can be explained by two components of texture coming from differently aligned domains with different cation stacking sequences in each domain: ABCABC... or ACBACB...., respectively (Fig. 4). Each domain generates a 3-fold symmetry in the {100} pole figure, and is separated by 60° around the surface normal (namely $c_{\perp 0}$ being in exact alignment with the substrate and $c_{\perp 60}$). The intensities are approximately the same for the 2 stacking sequences and the films consist of 2-equally-distributed components with the following (1) and (2) hetero-epitaxial relationships:

($c_{\perp 0}$) <001> $LiNbO_3$ // <001> Al_2O_3 and <100> $LiNbO_3$ // <100> Al_2O_3 (1)

($c_{\perp 60}$)<001> $LiNbO_3$ // <001> Al_2O_3 and <110> $LiNbO_3$ // <100> Al_2O_3 (2)

Because the Li cations are coordinated by 3 Nb cations, whenever Li moves, it creates cation disorder. Thus, it could be proposed that cation disorder, produced by the easier mobility of light Li cations at high temperatures, could cause all the variants to have a similar interfacial energy and, thus, no single variant would have any advantage to grow or disappear during deposition.

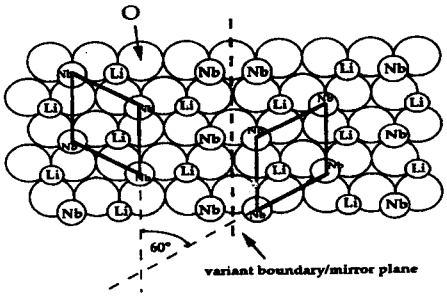

Fig. 4. Schematic showing 2 possible rotational variants of $LiNbO_3$ present on <00_1>-Al2O_3 (from [13])

Due to the pronounced formation of segregated 3-dimensional islands during the initial growth steps, both LN/Si and LN/Al_2O_3 heterostructures exhibit dense, homogeneous, columnar microstructures (Fig. 5). To minimize the film / substrate interface and, thus, reduce the interfacial energy, the crystallites grow with a reversed-pyramid shape.

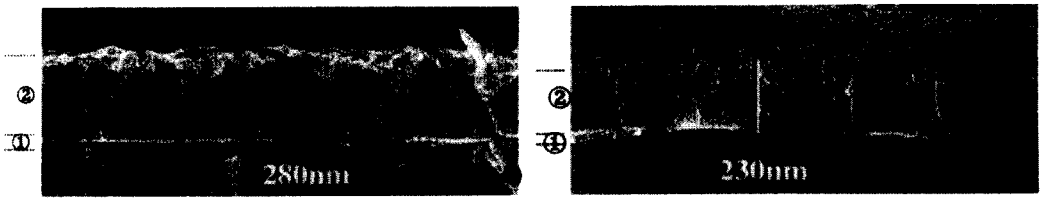

Fig 5. SEM micrographs of the cross section of $LiNbO_3$ thin films deposited on **(a)** <111>-Si and **(b)** <001> Al_2O_3 substrates.

Both (111)-Si and (001)-Al_2O_3 correspond to close-packed planes. Thus, when adsorbed on the surface of the substrates, the adatoms nucleate and form islands close-packed enough to (1)

prevent their in-plane spread during the coalescence step by limiting the lateral growth rate and (2) develop a columnar microstructure while keeping the same out-of-plane orientation (fastest growth direction perpendicular to the film surface).

Both the average grain size and surface roughness increase on Si in comparison with Al_2O_3 (Fig. 6). The lattice mismatch and difference of structure between LN and Si certainly create stresses within the films thus leading to grain boundary formation and grain boundary grooves which are significant contributors to grain growth and film roughening [13]. The use of semi-coherent interfaces, such as well-defined sapphire templates, allows a subsequent improve of the surface characteristics of the hetero-epitaxial films.

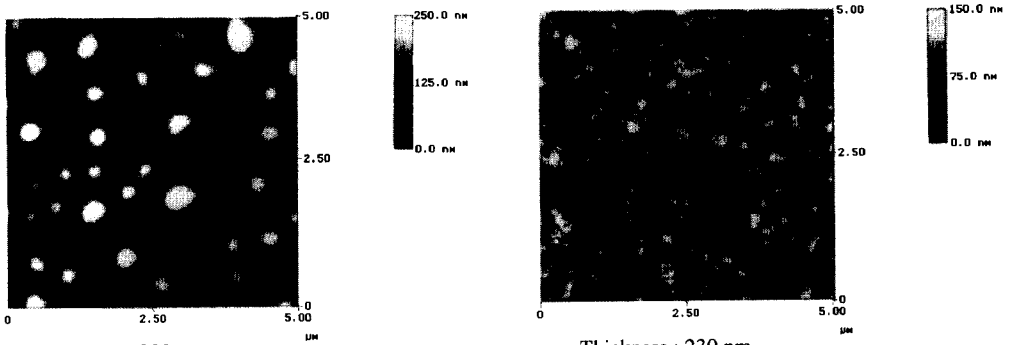

Fig 6. AFM micrographs of the $LiNbO_3$ thin films deposited on **(a)** <111>-Si and **(b)** <001> Al_2O_3 substrates.

Work is underway to study the SAW capabilities of such deposited samples. However, theoretical analysis of SAW propagation characteristics with inter-digital transducer (IDT) electrodes on top of the films has been performed to observe the effect of the underlying epitaxially-matched substrate. The results listed in Table 2 are an application of the theory of elastic wave propagation proposed by Farnell and Adler [14] and software developed by Fahmy and Adler [15].

Table 2. Coupling coefficients (k^2_{max}) and SAW velocity range for <c>-oriented $LiNbO_3$ films on <111>-Si and <001>-Al_2O_3 substrates.
(*f*: acoustic wave frequency; *e*: film thickness)

Substrate	**Film growth**	**Product (*f* x *e*)** (GHz.μm)	**K^2_{max}**	**Corresponding value of SAW velocity** (m/s)	**Maximal velocity (*f* x *e*=0)** (m/s)
Al_2O_3	<c>	3	0.42	3800	5600
Si	<c>	1.5	0.008	3800	4600

The use of Al_2O_3 underlying substrates is found to assist in waveguiding and enhances both the phase velocity values at low (*f* x *e*) product and the electromechanical coefficient. For high-frequency applications, growth of textured thin films is critical and can be achieved only on epitaxially-matching substrates. Considering the fact that the growth of thick defect-free textured layers remains challenging, one can figure out that appreciably high electromechanical coupling coefficient could be obtained at relatively low thickness values, thus making the LN/Al_2O_3 heterostructures good candidates for efficient high-frequency SAW devices.

Summary

By using a refined 2-step growth process – consisting of the combination of the r.f. sputtering and pyrosol techniques - highly <c>-preferred LN thin films can be successfully deposited on <111>-Si and <001>-Al_2O_3 substrates. If the former only exhibits a fiber texture, the latter well-evidences in-plane orientation of the crystallites with 2 separated main components.

Despite the good prospects of such as deposited materials, current investigations have yet to demonstrate their feasibility for SAW applications. Our work suggests that the device success is probably limited by the lack of in-plane organization in the films, rather than by intrinsic material parameters. We anticipate that ultimate device success can be achieved by improving the degree of texturation through the use of Al_2O_3 substrate and the control of its surface quality .prior to deposition.

Acknowledgements

This work has been funded by the European Union project under the Growth program (G6RD-CT99-00169) ESQUI: "X-ray Expert System for Electronic Films Quality Improvement".

References

[1] R.S. Wei, T.K. Gaylord: Appl. Phys. A37 (1985) 191.

[2] J. Lin, J. Chen, K.S. Ho, T.A. Rabson: Int. Ferr. 11 (1995) 221.

[3] J.T. Lee, N. Little, T. Rabson, M. Robert: IEEE Ultr. Symp. (1999) 269.

[4] S. Zhgoon, Q. Zhang, S.F. Yoon, A. Revkov, B. Gan, J.A; Rusli: Diamond and Related Materials 9 (2000) 1430.

[5] Y. Shibata, K. Kaya, K. Akashi, M. Kanai, T. Kawai, S. Kawai: J. Appl. Phys. 77 [4] (1995) 1498.

[6] V. Bornand, I. Huet, Ph. Papet, E. Philippot: Ann. Chim. Sci. Mat. 26 (2001) 49.

[7] H. Yoshiyama, S. Tanaka, Y. Hikami, S. Ohshio, J. Nishiura, H. Kawakami, H. Kobayashi: J. Cryst. Growth 56 (1988) 56.

[8] N. Fujimura, T. Nishira, S. Goto, J. Xu, T. Ito: J. Cryst. Growth 130 (1993) 269.

[9] J. Ricote, D. Chateigner, L. Pardo, M. Algueró, J. Mendiola, M.L. Calzada: Ferroelectrics 241 (2000) 167.

[10] H.-R. Wenk, S. Matthies, J. Donovan, D. Chateigner: J. Appl. Cryst. 31 (1998) 262.

[11] D.L. Smith, *Thin Film Deposition Principles and Practice* (Mc Graww Hill, New York, 1995) p. 327-380.

[12] Z. Lu, *PhD Thesis*, Standford University (1995) p. 107-114.

[13] D.K. Fork, F. Armani-Leplingard, J.J. Kingston, G.B. Anderson: Mater. Res. Symp. Proc. 392 (1985) 189.

[14] G.W. Farnell, E.L.Adler: *Physical Acoustic Principles and Methods Vol. 9* (ed. W.P. Mason and R.N. Thurston, Academic Press, New York and London, 1972) Chap. 2 p. 35.

[15] H. Fahmy, E.D. Adler: Proc. IEEE 122 (1975) 470.